Grossmanite, CaTi³⁺AlSiO₆, a new pyroxene from the Allende meteorite

CHI MA* AND GEORGE R. ROSSMAN

Division of Geological and Planetary Sciences, California Institute of Technology, Pasadena, California 91125, U.S.A.

ABSTRACT

Grossmanite, $Ca(Ti^{3+},Mg,Ti^{4+})AlSiO_6$ with an end-member formula $CaTi^{3+}AlSiO_6$, is a new member of the Ca clinopyroxene group, where the trivalent cations are dominant in the M1 site with Ti^{3+} being the dominant trivalent cation. It occurs as micrometer-sized crystals along with spinel and perovskite in a melilite host in Ca-,Al-rich refractory inclusions from the Allende meteorite. The mean chemical composition determined by electron microprobe analysis of the type material is (wt%) SiO_2 27.99, Al_2O_3 24.71, CaO 24.58, Ti_2O_3 10.91, TiO_2 6.68, MgO 4.45, Sc_2O_3 0.43, V_2O_3 0.19, ZrO_2 0.13, FeO 0.08, Cr_2O_3 0.03, sum 100.20. Its empirical formula calculated on the basis of 6 O atoms is $Ca_{1.00}[(Ti^{3+}_{0.35}Al_{0.18}Sc_{0.01}V^{3+}_{0.01})_{\Sigma0.55}Mg_{0.25}Ti^{4+}_{0.19}]_{\Sigma1.00}(Si_{1.07}Al_{0.93})_{\Sigma2.00}O_6$. Grossmanite is monoclinic, $C2/c$; $a = 9.80$ Å, $b = 8.85$ Å, $c = 5.36$ Å, $\beta = 105.62°$, $V = 447.70$ Å³, and $Z = 4$. Its electron back-scatter diffraction pattern is an excellent match to that of Ti^{3+}-rich pyroxene with the $C2/c$ structure. The five strongest calculated X-ray powder diffraction lines are [d spacing in Å, (I), hkl] 2.996 (100) ($\bar{2}21$), 2.964 (31) (310), 2.581 (42) (002), 2.600 (28) ($\bar{1}31$), 2.535 (47) (221). The name is for Lawrence Grossman, a cosmochemist at the University of Chicago.

Keywords: Grossmanite, $Ca(Ti^{3+},Mg,Ti^{4+})AlSiO_6$, $CaTi^{3+}AlSiO_6$, new mineral, Ti-rich pyroxene, refractory inclusion, Allende meteorite, carbonaceous chondrite

INTRODUCTION

During a nano-mineralogical investigation of the Allende meteorite (a CV3), Ti-rich pyroxenes were observed in Ca-,Al-rich refractory inclusions (CAI). Electron-microprobe, high-resolution SEM, electron backscatter diffraction (EBSD), and mico-Raman analyses have been used to characterize its composition and structure. Highly Ti-enriched clinopyroxenes (16–18 wt% total TiO_2) have been observed in Allende since its fall in 1969 (e.g., Fuchs 1971; Dowty and Clark 1973; Mason 1974; Simon et al. 1999). We report here the occurrence, composition and crystal symmetry of a clinopyroxene from Allende, $Ca(Ti^{3+},Mg,Ti^{4+})AlSiO_6$, where Ti^{3+} is the dominant trivalent component and the trivalent cations are dominant in the M1 site. The newly approved dominant-valency rule (Hatert and Burke 2008) is applied here to designate this pyroxene as a new mineral.

MINERAL NAME AND TYPE MATERIAL

The new mineral and its name have been approved by the Commission on New Minerals, Nomenclature and Classification (IMA 2008-042a). The name is for Lawrence Grossman, Professor of Cosmochemistry at the University of Chicago, born in 1946, in honor of his fundamental contributions to meteorite research. Type material (Caltech Section Allende12 MC2I) has been deposited in the Smithsonian Institution's National Museum of Natural History and is cataloged under USNM 7562.

OCCURRENCE, ASSOCIATED MINERALS, AND ORIGIN

Micrometer-sized grossmanite (the type material) occurs with $MgAl_2O_4$ spinel and $CaTiO_3$ perovskite in a melilite $[Ca_{2.00}(Al_{0.94}Mg_{0.07})(Si_{1.06}Al_{0.94})O_7]$ host in a CAI fragment from

* E-mail: chi@gps.caltech.edu

the Allende meteorite (Fig. 1). The inclusion with a Wark-Lovering rim is exposed in one polished thick section, prepared from a 1 cm Allende specimen at Caltech. This CAI fragment is 330×385 μm in the section plane, surrounded by a matrix of mostly olivine and troilite. The Allende meteorite, which fell at Pueblito de Allende, Chihuahua, Mexico, on February 8, 1969, is a CV3 carbonaceous chondrite.

Grossmanite is also observed in a Type B1 CAI from Allende in sections USNM 7554 and USNM 7555 (which were previously Caltech sections), occurring with spinel, perovskite, grossite in melilite near the rim, as shown in Figure 2.

APPEARANCE, PHYSICAL AND OPTICAL PROPERTIES

The type material (1–7 μm in size) appears to coat spinel grains (Fig. 1). In thin section, it is transparent with a light-gray color that may be caused by adjacent and underlying phases. Streak, luster, hardness, tenacity, cleavage, fracture, and density were not determined because of the small grain size. The density, calculated from the empirical formula, is 3.41 g/cm³. It is non-fluorescent under the beams of the electron microprobe and SEM. Optical properties were not determined because of the small grain size. In the section, the crystal grains are irregular. No crystal forms or twinning were observed. The $a:b:c$ ratio calculated from the unit-cell parameters is 1.107:1:0.606. Larger crystals of grossmanite in USNM 3848 (Dowty and Clark 1973) and Ti-rich diopside in TS32 (Simon et al. 1999) show a green color under oblique illumination.

CHEMICAL COMPOSITION

Quantitative elemental microanalyses were conducted with the JEOL 8200 electron microprobe operated at 15 kV and 10 nA in a focused beam mode. Standards for the analysis were
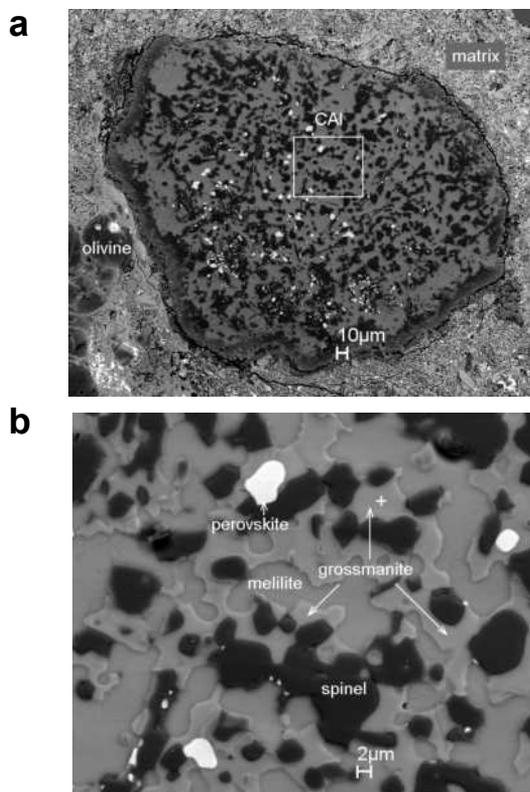
a

b

FIGURE 1. (**a**) Back-scatter electron image of the grossmanite-containing refractory inclusion in an Allende section (USNM 7562); (**b**) enlarged BSE image showing grossmanite with perovskite and spinel in a melilite host. The cross marks where the EBSD pattern (shown in Fig. 3) was collected.

anorthite (CaKα, AlKα, SiKα), TiO_2 (TiKα), synthetic forsterite (MgKα), V_2O_3 (VKα), $ScPO_4$ (ScKα), zircon (ZrLα), synthetic fayalite (FeKα), and Cr_2O_3 (CrKα). Analyses were processed with the CITZAF correction procedure (Armstrong 1995). Eight individual analyses of the type material reported in Table 1 were carried out using WDS mode. No other elements with atomic number greater than 4 were detected by WDS scans.

The empirical formula, based on 6 O apfu, is: $Ca_{1.00}[(Ti^{3+}_{0.35}Al_{0.18}Sc_{0.01}V_{0.01})_{\Sigma0.55}Mg_{0.25}Ti^{4+}_{0.19}]_{\Sigma1.00}(Si_{1.07}Al_{0.93})_{\Sigma2.00}O_6$, with Ti^{3+} and Ti^{4+} partitioned, based on stoichiometry. The general formula is $Ca(Ti^{3+},Mg,Ti^{4+})AlSiO_6$ and the end-member formula is $CaTi^{3+}AlSiO_6$, which requires Ti_2O_3 30.08, CaO 23.46, SiO_2 25.14, Al_2O_3 21.33, total 100.01 wt%.

Grossmanite from Type B1 CAI in USNM 7555 has an empirical formula $Ca_{1.01}[(Ti^{3+}_{0.28}Al_{0.16}Sc_{0.01}V_{0.01})_{\Sigma0.46}(Ti^{4+}_{0.28}Zr_{0.01})_{\Sigma0.29}Mg_{0.25}]_{\Sigma0.98}(Al_{1.01}Si_{0.99})_{\Sigma2.00}O_6$. The large green Ti-rich pyroxene in TS32 has a formula $Ca_{1.00}[Mg^{2+}_{0.46}(Ti^{3+}_{0.30}Al^{3+}_{0.06})_{\Sigma0.36}Ti^{4+}_{0.18}]_{\Sigma1.00}(Si_{1.28}Al_{0.72})_{\Sigma2.00}O_6$, which is not grossmanite, but Ti-rich diopside.

CRYSTALLOGRAPHY

Crystallography by EBSD at a sub-micrometer scale was carried out using the methods described in Ma and Rossman (2008, 2009a, 2009b) with an HKL EBSD system on the ZEISS 1550VP scanning electron microscope, operated at 20 kV and 6 nA in a focused beam with a 70° tilted stage. The structure was confirmed and cell constants were obtained by matching the experimental EBSD pattern (Fig. 3) with the structures of

Ti^{3+} pyroxene (Dowty and Clark 1973), synthetic $CaScAlSiO_6$ (Ohashi and Ii 1978), esseneite (Cosca and Peacor 1987), and orthorhombic pyroxenes (Molin 1989).

The EBSD patterns can be indexed only by the monoclinic $C2/c$ structure to give a best fit based on unit-cell data from Ti-rich pyroxene (Dowty and Clark 1973) (Fig. 3), showing a monoclinic structure, space group: $C2/c$, $a = 9.80$ Å, $b = 8.85$ Å, $c = 5.36$ Å, $\beta = 105.62°$, $V = 447.70$ Å^3, and $Z = 4$ with the mean angular deviations as low as 0.26. No errors are stated because the cell parameters are taken directly from the data of the matching phase in Dowty and Clark (1973). The Ti-rich pyroxene in USNM 3848 characterized by Dowty and Clark (1973) is grossmanite with a formula $Ca_{1.01}[(Ti^{3+}_{0.34}Al_{0.13})_{\Sigma0.47}Mg_{0.38}Ti^{4+}_{0.14}]_{\Sigma0.99}(Al_{1.26}Si_{0.74})_{\Sigma2.00}O_6$.

X-ray powder-diffraction data ($CuK\alpha_1$) are calculated from the cell parameters from Dowty and Clark (1973) with the empirical formula of the type grossmanite from this study (Table 1) using Powder Cell version 2.4 (2000). The strongest X-ray powder diffraction lines are [d spacing in Å, (I), hkl] 2.996 (100) ($\overline{2}$21), 2.964 (31) (310), 2.909 (25) ($\overline{3}$11), 2.581 (42) (002), 2.600 (28) ($\overline{1}$31), 2.535 (47) (221), 2.130 (19) ($\overline{3}$31), 1.650 (18) ($\overline{2}$23), 1.431 (19) (531).

SPECTROSCOPIC PROPERTIES

Raman microanalysis was carried out using the methods described in Ma and Rossman (2008, 2009a). Raman analysis gave
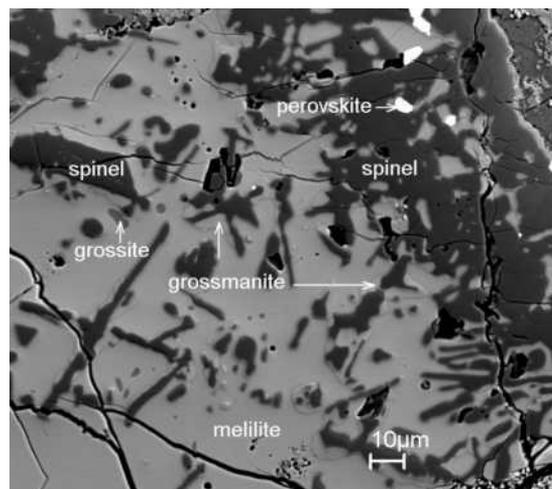

FIGURE 2. BSE image showing grossmanite with spinel, perovskite, and grossite in melilite near the rim of a type B1 CAI in USNM 7555.

TABLE 1. The mean electron microprobe analytical results for the type grossmanite

Constituent	wt%	Range	Std. dev.	EPMA standard
SiO_2	27.99	27.50–28.60	0.32	anorthite
Al_2O_3	24.71	24.39–25.39	0.30	anorthite
CaO	24.58	24.32–24.81	0.18	anorthite
Ti_2O_3*	10.91	10.72–11.10	0.13	TiO_2
TiO_2*	6.68	6.56–6.79	0.08	TiO_2
MgO	4.45	4.21–4.66	0.15	Mg_2SiO_4
Sc_2O_3	0.43	0.38–0.48	0.03	$ScPO_4$
V_2O_3	0.19	0.17–0.23	0.02	V_2O_3
ZrO_2	0.13	0.07–0.19	0.04	zircon
FeO	0.08	0.00–0.15	0.05	Fe_2SiO_4
Cr_2O_3	0.03	0.00–0.04	0.02	Cr_2O_3
Total	100.20			

* Total titanium, which equals 18.80 wt% as TiO_2, has been partitioned between Ti^{3+} and Ti^{4+} to make ideal stoichiometry.
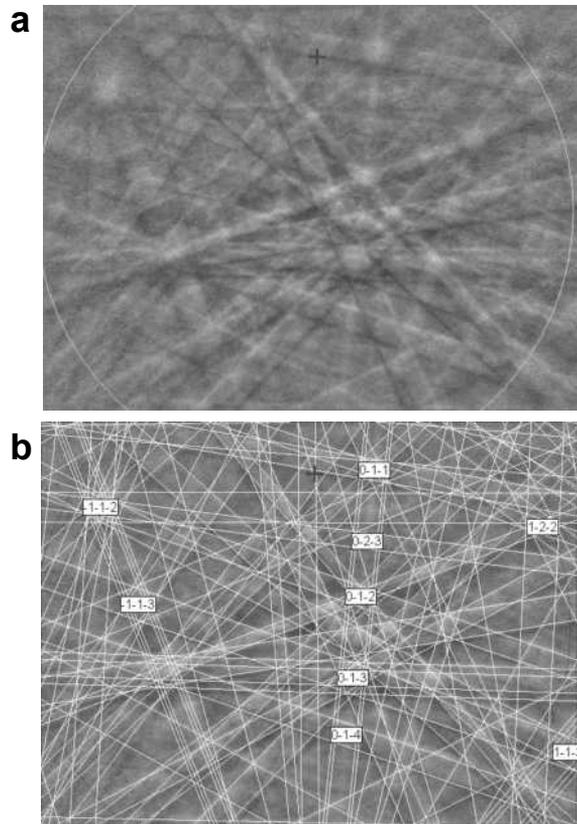
FIGURE 3. (**a**) EBSD pattern of the labeled grossmanite crystal (marked with a cross) in Figure 1b; (**b**) the pattern indexed with the *C*2/*c* pyroxene structure.

no indication of either H_2O or CO_2 in grossmanite. Raman microanalyses show that the spectra of grossmanite (using a 514.5 nm laser) in USNM 7555 are close to those of Ti-rich diopside in TS32 and esseneite (RRUFF -R061123) (see supplemental figure[1] on deposit), whereas the spectrum of the type grossmanite in USNM 7562 shows numerous fluorescence features in the 1500 to 900 cm^{-1} and some in the 900–200 cm^{-1} region due either to likely traces of REE in the structure or coming from signal spillover from adjacent phases such as perovskite.

Optical absorption spectra (Fig. 4) indicate that grossmanite and Ti-rich diopside from Allende contain a significant amount of Ti^{3+} in the structure that causes the green color. The dominant absorption features are a rising absorption toward shorter wavelength with two superimposed absorption bands at 490 and 608 nm. Previous studies of a pyroxene from the Allende meteorite (Dowty and Clark 1973) have demonstrated that Ti^{3+} in the pyroxene's M1 site produces optical absorption bands centered at nearly the same wavelengths (490 and 606 nm) in a sample with much lower Ti content. Other synthetic Ti^{3+}-containing pyroxenes of somewhat different composition have been studied and were found to have a pair of bands at somewhat

longer wavelengths than the Allende pyroxenes. Skogby et al. (2006) examined the optical absorption spectrum of a series of synthetic, Ti-doped diopside samples and found two bands centered at 547 and 637 nm that correlated with the amount of Ti^{3+}. In addition, an optical absorption spectrum of a sample of synthetic $NaTi^{3+}Si_2O_6$ (GRR216) synthesized by RD Shannon (Prewitt et al. 1972) was obtained (Fig. 4). It also had a pair of absorption bands (540 and 625 nm) intermediate between those of the diopsidic titanian pyroxene of Skogby et al. (2006) and grossmanite samples, and essentially identical to the spectrum of the same compound reported by Skogby et al. (2006) where they report bands at 547 and 637 nm.

Ti^{4+}, by itself, has an empty *d*-orbital electronic configuration and is incapable of causing optical absorption in the visible range. Fe^{2+}-Ti^{4+} intervalence charge transfer produces only a single band at lower wavelengths in pyroxenes (Mao et al. 1977).

A crude estimate of the amount of Ti^{3+} in grossmanite can be established using the intensity of the Ti^{3+} absorption in the $NaTi^{3+}Si_2O_6$ spectrum reported by Skogby et al. (2006) who observe a Ti^{3+} band intensity of about 120 per cm at 15 700 cm^{-1} for the M1 site completely occupied by Ti^{3+}. The corresponding band in the grossmanite spectrum has an intensity of about 12 per cm corresponding to minimum of about 0.18 of a site occupied by Ti^{3+}. This estimate is a minimum because the grossmanite crystal was not oriented in a direction to obtain an optimal polarization direction. Nevertheless, this estimate compares favorably with the 0.348 apfu from the empirical formula determined from the electron-probe analysis. While the exact intensity of Ti^{3+} absorption in grossmanite is unknown, this estimate demonstrates a substantial amount of Ti^{3+} in this phase.

DISCUSSION

Grossmanite is a new member of the Ca clinopyroxenes (diopside group) with space group *C*2/*c*, the Ti^{3+}-dominant analog of esseneite ($CaFe^{3+}AlSiO_6$) (Cosca and Peacor 1987), davisite ($CaScAlSiO_6$) (Ma and Rossman 2009b), kushiroite (CaTs pyroxene, $CaAlAlSiO_6$) (Kimura et al. 2009; Ma et al. 2009), where the trivalent cations are dominant in the M1 site with Al occupying about 50% of the tetrahedral Si site. As shown in Figure 5, there seems to be a solid solution among diopside,
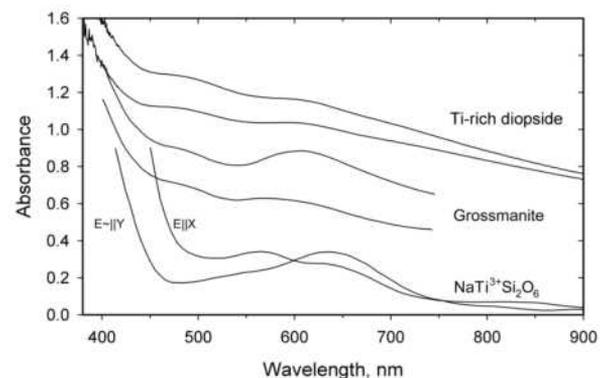

FIGURE 4. Optical absorption spectra of a 52 μm thick Ti-rich diopside in TS32 (this study), grossmanite in USNM3848 of unspecified thickness (Dowty and Clark 1973), and a 30 μm thick synthetic $NaTi^{3+}Si_2O_6$ pyroxene (GRR216). The Ti-rich diopside and grossmanite are polarized in two extinction directions in the section plane. Each pair of spectra has been displaced vertically for clarity.
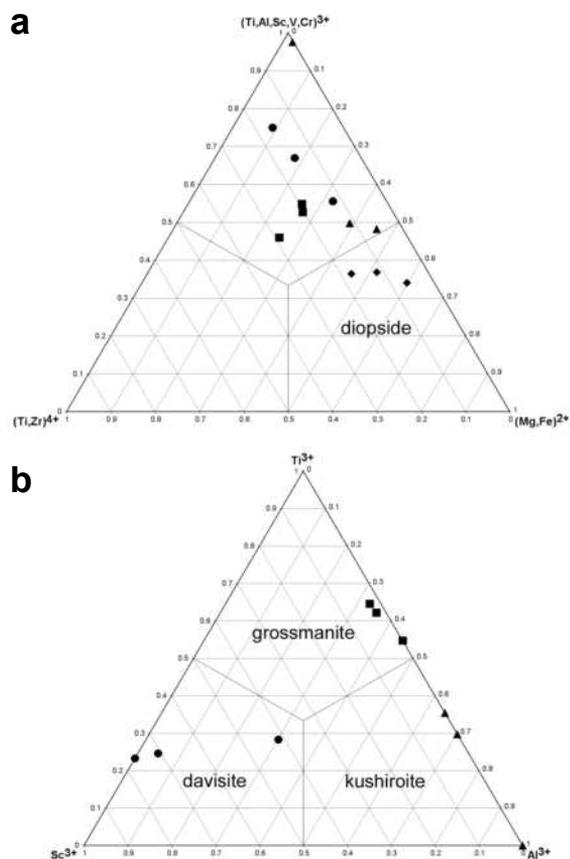
FIGURE 5. (**a**) Molar ternary diagram of three cation groups in the M1 site from the Allende clinopyroxenes of this study, Ma and Grossman (2009b) and Ma et al. (2009); (**b**) normalized ternary diagram of Ti^{3+}-Sc^{3+}-Al^{3+} from the same clinopyroxenes where the trivalent cations are dominant in the M1 site. Square = grossmanite (USNM 7562, 7555, 7554); circle = davisite (USNM 7555); triangle = kushiroite (USNM 7554; ALH1); diamond = Ti-rich diopside (USNM 7554, TS32).

grossmanite, davisite, and kushiroite based on this study and on Ma and Grossman (2009b) and Ma et al. (2009).

Term "fassaite" refers to Ti-bearing and Al-rich Ca clinoproxene in refractory inclusions from chondrites (Dowty and Clark 1973; Brearley and Jones 1998), which is well known and widely used in the meteoritics community, although the name was discredited officially by the IMA-CNMNC (Morimoto et al. 1988). By definition, Ti-rich "fassaite" pyroxenes are grossmanite if trivalent cations are dominant in the M1 site with Ti^{3+} being the dominant trivalent cation (Fig. 5). If trivalent cations dominate the M1 site with Sc^{3+} the dominant trivalent cation, such "fassaite" is davisite. When trivalent cations dominate the M1 site with Al the dominant trivalent cation, the "fassaite" is kushiroite. If Mg^{2+} is dominant in the M1 site, the "fassaite" is diopside.

The Allende meteorite containing 0.15 wt% total TiO_2 (Jarosewich et al. 1987) has provided a variety of phases with high titanium contents including oxides, pyroxenes, perovskite, and zirconolite as primitive refractory phases. Grossmanite and Ti-rich diopside often have Ti in both 3+ and 4+ oxidation states. Such pyroxenes formed in a reducing environment (Beckett 1986). Another newly discovered mineral tistarite (Ti_2O_3, IMA 2007-027) from Allende is the most Ti^{3+}-rich mineral in nature

(Ma and Rossman 2009a). Refractory phases are the first known solids formed in the solar system. Grossmanite is a refractory mineral from Allende, associated with Mg-Al spinel, perovskite, and melilite in CAIs, which are likely formed through high-temperature condensation in the solar nebula, followed by melting and crystallization. Grossmanite apparently formed after the appearance of spinel and perovskite but before crystallization of melilite in the type material setting.

REFERENCES CITED

Armstrong, J.T. (1995) CITZAF: A package of correction programs for the quantitative electron microbeam X-ray analysis of thick polished materials, thin films, and particles. Microbeam Analysis, 4, 177–200.

Beckett, J.R. (1986) The origin of calcium-, aluminum-rich inclusions from carbonaceous chondrites: an experimental study, 373 p. Ph.D. thesis, University of Chicago.

Brearley, A.J. and Jones, R.H. (1998) Chondritic meteorites. In J.J. Papike, Ed., Planetary Materials, 36, p. 3-1–3-398. Reviews in Mineralogy, Mineralogical Society of America, Chantilly, Virginia.

Cosca, M.A. and Peacor, D.R. (1987) Chemistry and structure of esseneite ($CaFeAlSiO_6$), a new pyroxene produced by pyrometamorphism. American Mineralogist, 72, 148–156.

Dowty, E. and Clark, J.R. (1973) Crystal structure refinement and optical properties of a Ti^{3+} fassaite from the Allende meteorite. American Mineralogist, 58, 230–242.

Fuchs, L.H. (1971) Occurrence of wollastonite, rhonite, and andradite in the Allende meteorite. American Mineralogist, 56, 2053–2068.

Hatert, F. and Burke, E.A.J. (2008) The IMA-CNMNC dominant-constituent rule revised and extended. Canadian Mineralogist, 46, 717–728.

Jarosewich, E., Clarke Jr., R.S., and Barrows, J.N. (1987) The Allende meteorite reference sample. Smithsonian Contributions to the Earth Sciences, No. 27.

Kimura, M., El Goresy, A., Mikouchi, T., Suzuki, A., Miyahara, M., and Ohtani, E. (2009) Kushiroite, $CaAl_2SiO_6$, a new mineral in carbonaceous chondrites: its formation conditions and genetic significance in Ca-Al-rich Refractory inclusions. 72nd Annual Meteoritical Society Meeting, abstract 5174.

Ma, C. and Rossman, G.R. (2008) Barioperovskite, $BaTiO_3$, a new mineral from the Benitoite Mine, California. American Mineralogist, 93, 154–157.

——— (2009a) Tistarite, Ti_2O_3, a new refractory mineral from the Allende meteorite. American Mineralogist, 94, 841–844.

——— (2009b) Davisite, $CaScAlSiO_6$, a new pyroxene from the Allende meteorite. American Mineralogist, 94, 845–848.

Ma, C., Simon, S.B., Rossman, G.R., and Grossman, L. (2009) Calcium Tschermak's pyroxene, $CaAlAlSiO_6$, from the Allende and Murray meteorites: EBSD and micro-Raman characterizations. American Mineralogist, 94, 1483–1486.

Mao, H.K., Bell, P.M., and Virgo, D. (1977) Crystal field spectra of fassaite from the Angra dos Reis Meteorite. Earth and Planetary Science Letters, 35, 353–356.

Mason, B. (1974) Aluminum-titanium-rich pyroxenes, with special reference to the Allende meteorite. American Mineralogist, 59, 1198–1202.

Molin, G.M. (1989) Crystal-chemical study of cation disordering in Al-rich and Al-poor orthopyroxenes from spinel lherzolite xenoliths. American Mineralogist, 74, 593–598.

Morimoto, N., Fabries, J., Ferguson, A.K., Ginzburg, I.V., Ross, M., Seifert, F.A., Zussman, J., Aoki, K., and Gottardi, G. (1988) Nomenclature of pyroxenes. American Mineralogist, 73, 1123–1133.

Ohashi, H. and Ii, N. (1978) Structure of calcium scandium aluminum silicate ($CaScAlSiO_6$)-pyroxene. Journal of the Japanese Association of Mineralogists, Petrologists and Economic Geologists, 73, 267–273.

Prewitt, C.T., Shannon, R.D., and White, W.B. (1972) Synthesis of a pyroxene containing trivalent titanium. Contributions to Mineralogy and Petrology, 35, 77–82.

Simon, S.B., Davis, A.M., and Grossman, L. (1999) Origin of compact type A refractory inclusions from CV3 carbonaceous chondrites. Geochimica et Cosmochimica Acta, 63, 1233–1248.

Skogby, H., Hålenius, U., Kristiansson, P., and Ohashi, H. (2006) Titanium incorporation and $^{VI}Ti^{3+}$-$^{IV}Ti^{4+}$ charge transfer in synthetic diopside. American Mineralogist, 91, 1794–1801.